Teaching assistant
Valentin Rougier
EPFL LPAC – MXH 144
valentin.rougier@epfl.ch

LCM & PERMEABILITY

Location
MED 3 1119

Note: all relevant values are given in Table 1.
Optionally, read the annexes and pages 5–10 for further information on LCM.

Goals

In this TP, we will show why the concept of permeability plays an important role in impregnation for liquid composite molding processes (LCM), and how it can be measured. Using a simplified setup for RTM (Resin Transfer Molding), which is a particular case of LCM, we will discuss the links between the resin velocity v, the permeability K of reinforcements and the presence of defects in the resulting parts.

Our goal here will be to measure the longitudinal permeability of a compressed stack of fabric. Since we are solely interested in impregnation, we will use silicon oil as a test liquid, which will not solidify in this experiment. The permeability will be assessed in single-phase *("saturated")* and two-phase *("unsaturated")* flow configurations from a 2-steps experiment, following the guidelines in the annexes:

- Emulate and monitor the impregnation step in a RTM process
- Prepare the fabric and the experimental setup
- Record the evolution of the flow front position
- Measure the liquid flow rate when it is fully saturated
- Analyze the results and determine the 1D longitudinal permeability of the fabric
- Compare the permeability K_{sat} measured in the *saturated* configuration (single-phase flow), and K_{unsat} measured in the *unsaturated* configuration (two-phase flow)

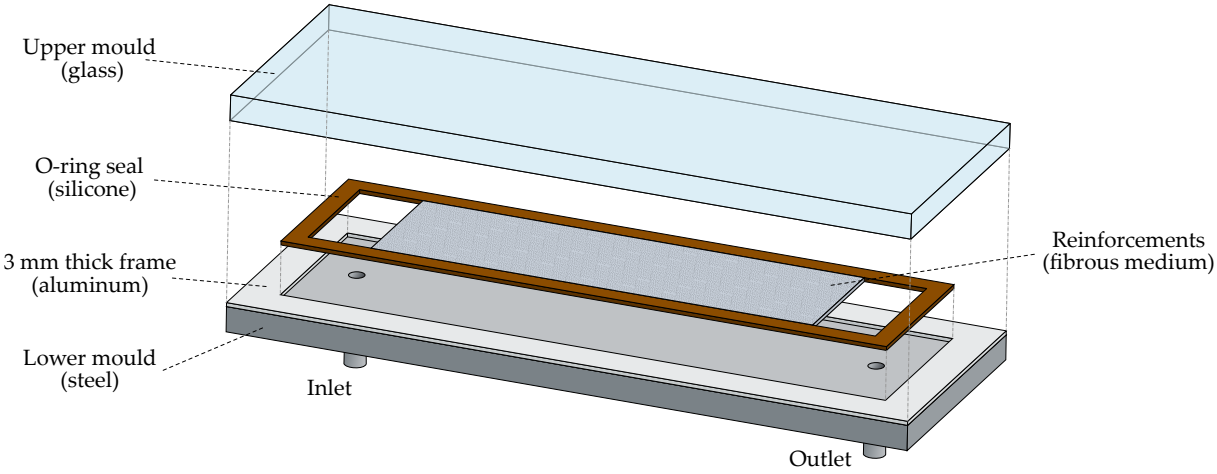

FIGURE 1: Schematic of the mould setup

Experimental procedure

Fabric and mould preparation

- Open and clean the mould. Make sure markings are still present.
- Calculate the number n of fabric layers needed to get $V_f = n\sigma/(\rho h) = (35 \pm 3)\,\%$ — use the thickness h of the mould frame and the fabric properties ρ, σ given in Table 1.
- Cut the fabric into n rectangles of $350\,\text{mm} \times 100^{+1}_{-0}$ mm.
  Check that they fit the mould perfectly: there should be no empty space on the sides.
- Weigh the fabric stack to determine the precise fiber volume fraction V_f.
- Place the metallic frame , the silicon O-ring seal and the fabric according to Figure 1.
- Close the mould, **place the pins** and apply a pressure of $\sim 3.5\,\text{bar}$ to compress the fibers.
- Prepare the pressure pot (check that there is enough liquid left). With the valve closed, apply a pressure of approximately 700 mbar (70 kPa).
- Place the camera, set its focus on the fabric.
- Ensure that the mass acquisition program runs without errors.

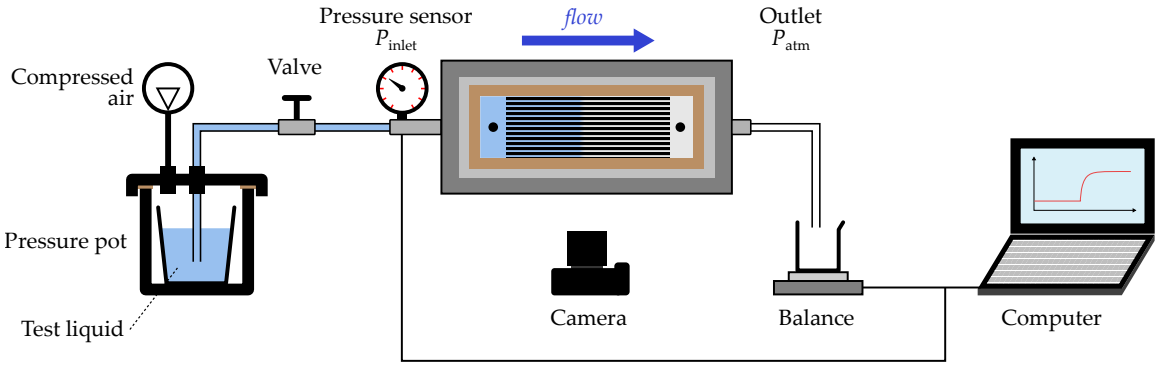

FIGURE 2: Schematic of the permeability measurement setup

Injection of the test fluid

- Start the video (camera) and pressure acquisition (PC) simultaneously and open the valve.
- Let the camera record the flow front position $x(t)$ during impregnation (unsaturated/two-phase flow) and then stop the video.
- Record the mass $m(t)$ of outcoming fluid (saturated/single-phase flow) for a couple of minutes.

Data analysis

The experimental data will be provided after the TP. It comprises the video of the flow front, the recording of pressure $\Delta P(t)$, and the mass of liquid $m(t)$ recorded by the balance.

Two-phase flow configuration

Analyze the experimental data (video and pressure datasheet) according to annex II (*"Experimental Procedures to Run Longitudinal Injections to Measure Unsaturated Permeability of LCM Reinforcements"*, paragraph 8.2):

- Plot the evolution of the square of the flow front position $x^2(t)$ and find its slope.

- Determine the average pressure difference ΔP between the outlet and the inlet.
- Deduce the permeability K_{unsat} from experimental data.

Single-phase flow configuration

Calculate the permeability K_{sat} according to annex II (*"Permeability properties of reinforcements in composites"*, eq. 14.22):

- Plot $m(t)$ and its slope $\frac{\mathrm{d}m}{\mathrm{d}t}$. Deduce the average *volumetric* flow rate $Q = \frac{\mathrm{d}\mathcal{V}}{\mathrm{d}t}$.
- Calculate the corresponding permeability K_{sat}

Report

Write a short report of the whole TP **(maximum 10 pages)** in French or in English. Make sure to report all measurements and check for significant figures. Try plotting the data when it is relevant, and pay attention to the plot layouts. The following items should be included in the report, following the order that suits you the best while remaining logical:

- *Short* general introduction on the context of RTM (principles, applications, issues, etc.).
- Context on permeability (why is it important for RTM, definition, equations, etc.).
  Exercise: deduce the theoretical liquid velocity $v(t)$ in unidirectional flow at constant applied pressure by integrating Darcy's law (Equation 1):

$$v = \frac{\mathrm{d}x}{\mathrm{d}t} = -\frac{K}{\eta(1 - V_f)}\frac{\Delta P}{x} \tag{1}$$

- Explain what was done in this TP: goal, motivation, methods, results, analysis.
  - Compare the theoretical flow front velocity $v(t)$ with your measurements.
  - Compare the two methods for measuring permeability.
  - Calculate the ratio $R = K_{\text{unsat}}/K_{\text{sat}}$ and discuss its value (why?).
- Write a short conclusion.

The main point of the report is to show that you understand the subject, the experiment and how they relate to each other.

Parameters & values

Some of the parameters needed in order to calculate K are summed up in Table 1. The areal density of fabrics σ might differ slightly in the experiments. The fabric used during the TP should be the flax fabric, but a glass mat could also be used depending on their availability.

h_{mould} [mm]	η [Pa · s]	ρ_{liq} [kg/m^3]	ρ_{glass} [kg/m^3]	σ_{glass} [g/m^2]	ρ_{flax} [kg/m^3]	σ_{flax} [g/m^2]
3	0.1	965	2600	500	1450	300

TABLE 1: Other experimental parameters

Hints

How can one evaluate a slope?

Perform a regression analysis on the data. Many different software packages can do it, generally by least squares fitting using optimization routines, such as the Levenberg-Marquardt algorithm:

- Microsoft Excel provides the function LINREG (French: *DROITEREG*) which is suitable for linear regression, and can also easily be added to graphs.
- SciPy (python module) has multiple options available in its `optimize` submodule, such as `lsq_linear` or `curve_fit`.
- Gnuplot, with the command `fit`.
- ... and many more!

Data treatment and format

The pressure data given after the TP is the difference between measured pressure and atmospheric pressure P_{atm} at all acquisition times. It is given as a `.csv` file which can be opened and treated with MS Excel. The inlet pressure is given in column `CH1`, and time in columns `Date&Time` and `ms`.

Aspect of the pressure field

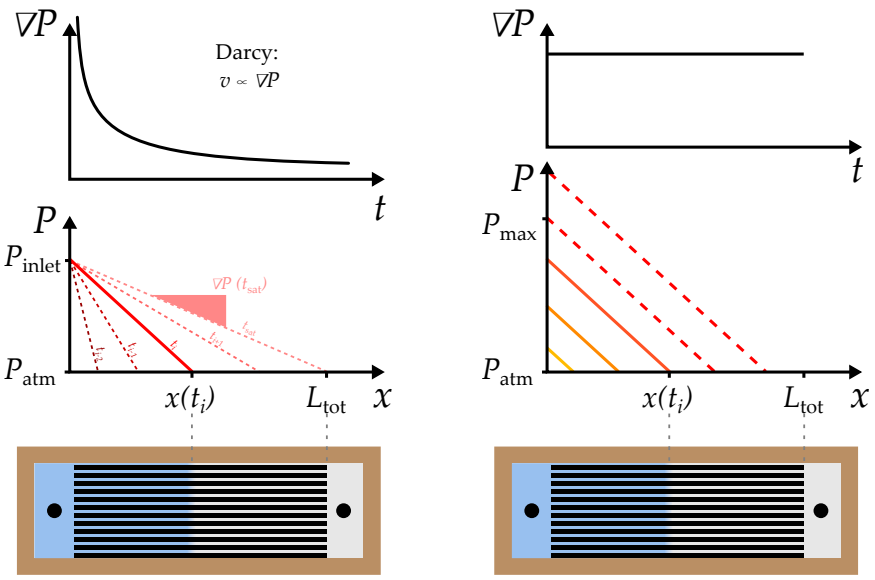

FIGURE 3: Idealized shape of the pressure field $P(x)$ for impregnations performed at a constant inlet pressure (left) and constant flow rate (right).

References

[1] J. Alms, N. Correia, S. Advani, and E. Ruiz. *Experimental procedures to run longitudinal injections to measure unsaturated permeability of LCM reinforcements*. FCPM Collaboration, 2010.

[2] V. Michaud. "Permeability properties of reinforcements in composites". In: *Composite Reinforcements for Optimum Performance*. Ed. by P. Boisse. Woodhead Publishing Series in Composites Science and Engineering. Woodhead Publishing, 2011, pp. 431–457. ISBN: 978-1-84569-965-9. DOI: 10.1533/9780857093714.3.431.

If you want to go further...

Here, we will introduce some details and phenomena which were not discussed so far, but tend to complicate the modeling of liquid composite molding processes. **These more advanced notions are not required in this TP, but may help you understand some limits of the simplified model we used here**. Indeed, several physical effects have to be accounted for depending on materials and processing conditions.

Capillarity and flow front dynamics

When deformable/soft interfaces are present (2-phase flow – in general, liquid/gas interfaces), capillary forces appear. Capillarity depends on surface tension γ and on the curvature of these interfaces: a curved interface is then associated with a force. The force resulting from the mean curvature of the whole interface is then balanced at the triple line (junction with the solid phase), and forms a contact angle θ.
In LCM, the triple line is where liquid, gas and fibers meet (Figure 4). Within the tows, the specific surface of fibers is very high ($1{\times}10^5$ to $1{\times}10^6$ m^2/m^3). Therefore, the total length of the triple line is large, and capillary forces tend to be highest in the tows.

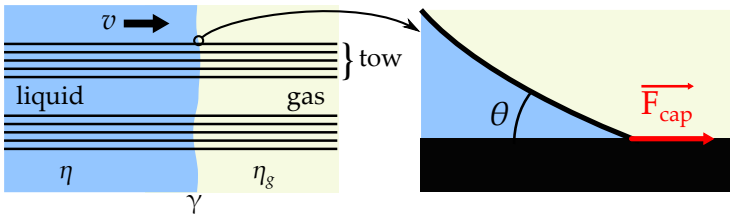

FIGURE 4: Capillary forces in LCM

A simplified way to model the problem at the macroscopic scale is to consider that the liquid/gas interface is localized at one specific distance $x(t)$ within the mould (think of a Dirac $\delta(x)$ function). In this case, the capillary forces should only apply there, and they can be summed up by a capillary pressure P_{cap} (Figure 5).

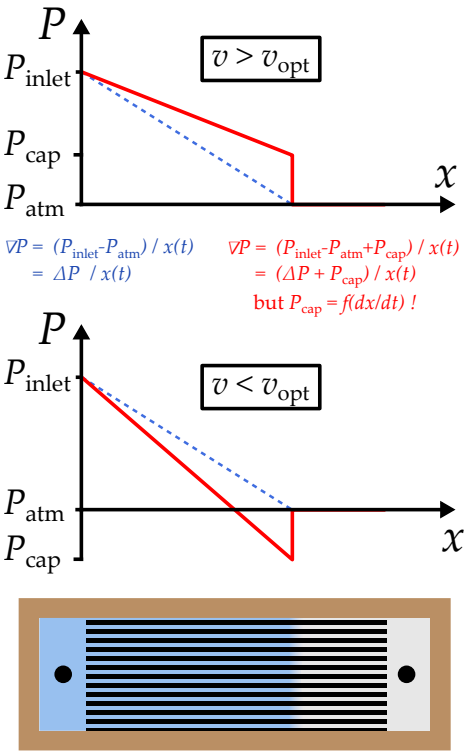

FIGURE 5: Simplified shape of the pressure field at a constant applied pressure, considering the capillary pressure P_{cap}.

Capillary pressure depends on the specific surface of fibers, surface tension, and contact angle. However, the value of the contact angle depends on the contact line velocity (*dynamic wetting*) [5]. This means that capillary pressure is a dynamic quantity, which affects the pressure field differently when the resin velocity changes. Researchers relate these capillary phenomena to the nondimensional capillary number $\mathrm{Ca} = \eta v/\gamma$, which represents the ratio of viscous and capillary forces, and is also proportional to the velocity.

For liquid composite molding processes, these considerations have important implications on parts quality. When the fluid velocity v is low, capillary pressure tends to favor the flow within the tows (see Figure 5: the more "negative" value of P_{cap} increases the pressure gradient, and thus the velocity according to Darcy's law). In such situations, lateral flows may trap large bub-

bles between the tows. When these bubbles are not removed, they end up forming voids in the composite part. The opposite phenomenon occurs at large flow velocities/capillary numbers: small voids are then trapped in the tows. Figure 5 shows the relation between void content in the parts and capillary number. One finds a range of Ca which minimizes voids; unfortunately, this value is difficult to predict and depends on the material properties and flow conditions. The relation between contact line velocity and contact angle is still not well elucidated, as it implies multiple length scales and various physical phenomena [13, 3]. These factors explain why this topic is still an active research subject [8, 12, 14].

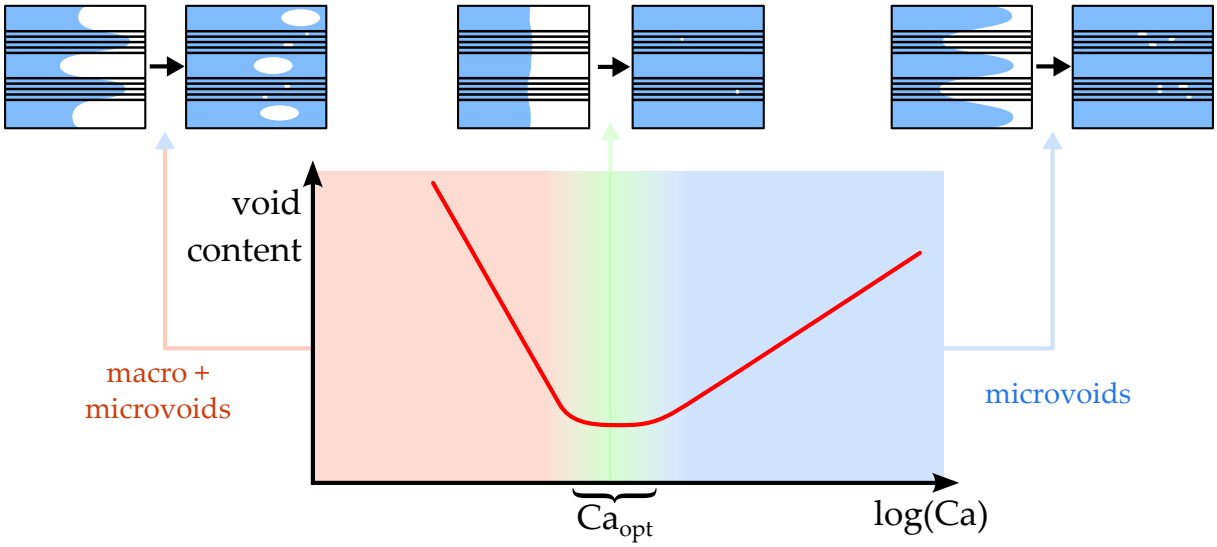

FIGURE 6: Relation between Ca ($\propto v$) and void content, and the associated phenomena

Saturation and shape of the flow front

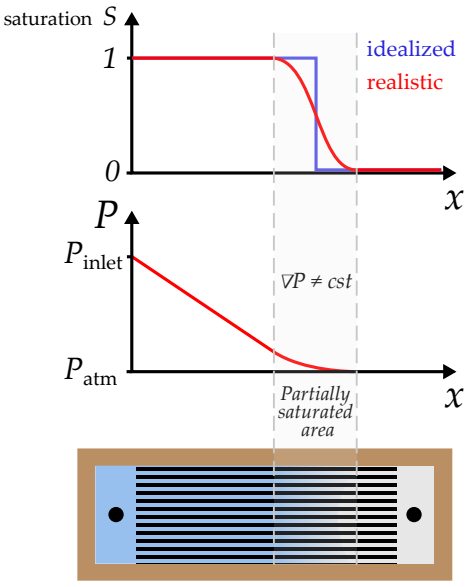

FIGURE 7: Example of a pressure field shape with a partially-saturated area at the front

In the previous section, we assumed that the flow front should be modeled as a sharp interface. This is rarely (if ever) observed in experiments: the flow front itself is diffuse, and not necessarily straight across the width of the mould. This can be modeled with the notion of *saturation* S, which is the ratio of available space occupied by the liquid. Figure 7 shows how a diffuse flow front results in the smearing of the saturation profile.

Experiments have shown that the areas partially saturated in resin are associated with concave or convex pressure fields [10]. The concavity or convexity is hypothesized to stem from capillarity. Depending on the flow conditions, capillary pressure can either help or hinder the resin flow. At mesoscopic scales, the link between capillarity and the spatial extent of the flow front can also be understood by looking at the schematics in Figure 6: capillarity is responsible for staggered flow front positions within and between the tows. Macroscopically, this results in an more smeared out saturation profile.

When capillary effects are neglected by models, their influence tends to be (incorrectly) reported on permeability. As such, the notion of *unsaturated permeability* can be found in the literature. This TP shows how this modeling shortcoming leads to two different measured

values of permeability.

Multiphase flow approach

So far, we have presented idealized situations where the resin fills the entire available space between the fibers. In most cases however, air pockets are trapped and affect the flow. Other modeling approaches try to consider that the two fluid phases can be present over the whole domain. This two-phase flow approach, which is popular in earth and soil science, accounts for the possible presence of the two fluids at every location in the porous medium by using the saturation S_α in each phase α. As an extension of Darcy's law, it is a macroscopic model which does not describe the details of the flow, but involves averaged values.

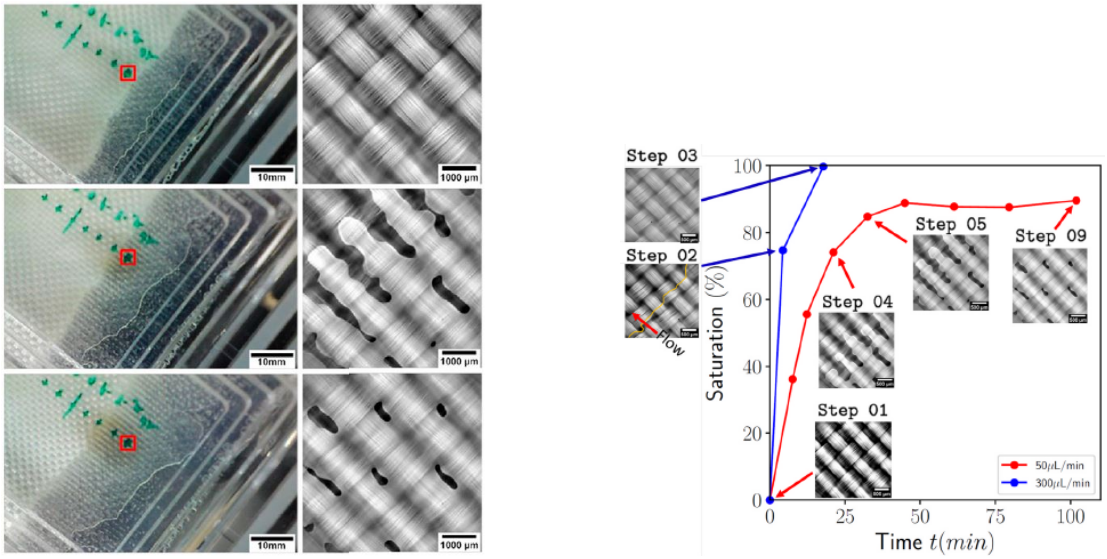

FIGURE 8: Xray images of fabric impregnation (left) and corresponding saturation profiles (right) [4].

In this family of models, permeability depends on the local saturation of each fluid. Therefore, the concept of *relative permeability* k_r is often used. The models also require additional closure relations between saturation, capillary pressure and relative permeabilities in order to be well-posed. A general formulation is given in Equation 2, which must be written for each phase α.

$$\begin{cases} \phi S_\alpha v_\alpha = -\dfrac{k_{r,\alpha}\, K}{\eta_\alpha} \nabla P_\alpha \\ \dfrac{\partial \phi S_\alpha}{\partial t} = -\nabla \cdot (\phi S_\alpha v_\alpha) \\ S_\alpha = f_2(P_{\text{cap}}) = f_2(P_\beta - P_\alpha) \\ k_{r,\alpha} = f_1(S_\alpha) \end{cases} \tag{2}$$

This modeling approach still comes with different issues, such as the physical meaning and well-posedness of some terms and relations. For instance, it has been shown that they do not account well for dynamic effects. There are also different semi-empirical models for expressing the hydraulic relations between S_α, $k_{r,\alpha}$ and P_{cap}, hence the notation f_1 and f_2 given here.

Sensitivity to environmental conditions

Some materials show a dependence on environmental conditions such as humidity and temperature. This is particularly true for natural fibers, which are often used nowadays for composite manufacturing. These fibers can degrade quickly at low temperatures (200 °C), which makes some processes hardly suitable. They also tend to be extremely hygrophilic, retaining moisture from air, and can also absorb water and resin during impregnation. This results in many potential issues, such as a variation of density, fiber swelling, poor adhesion or damage from sorption/desorption cycles. This also means that processes need to be adapted to optimize their use.

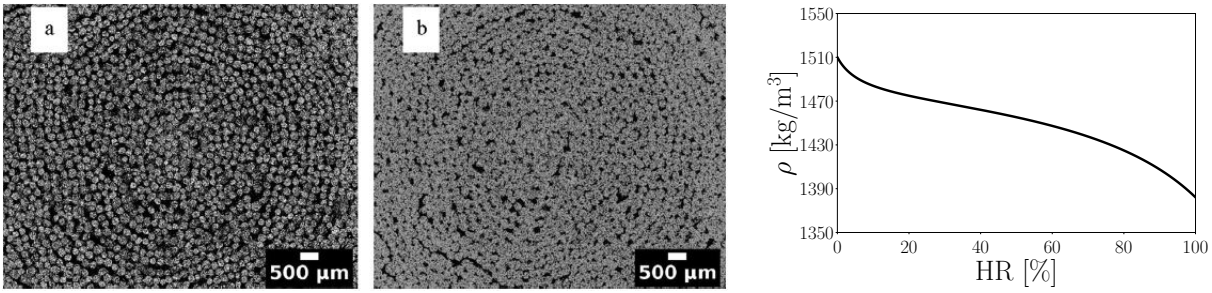

FIGURE 9: Cross-section of a flax yarn *a)* before and *b)* after water intake [15]; right: evolution of flax density with the relative humidity of air at thermodynamic equilibrium [11].

Models for permeability prediction

Permeability is actually a purely geometric quantity, and solely stems from the spatial configuration of the porous medium. In Darcy's law, it relates how this geometry induces viscous losses. Multiple models attempt to determine permeability by using mathematical descriptors of the porous medium: porosity, pore shape, pore tortuosity, connectivity... Due to the complexity of most porous media however, these quantities can only be estimated statistically [1, 2]. Some examples of commonly used models include the Kozeny-Carman model, Ergün's equation, and Gebart's model for fibrous media.

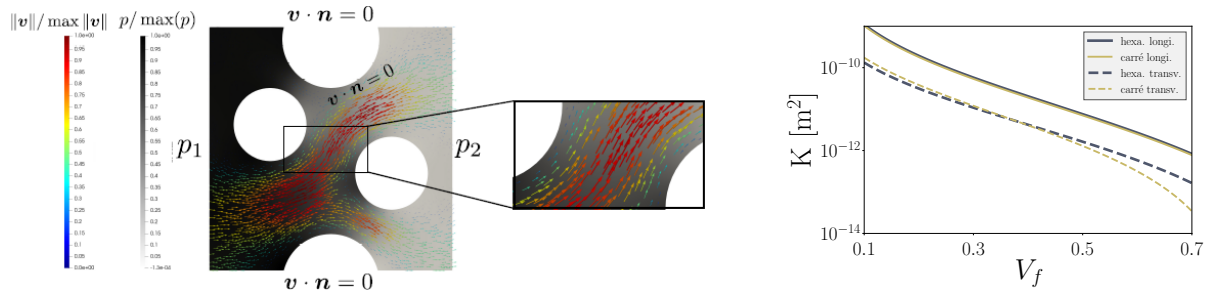

FIGURE 10: Permeability prediction via *(left)* numerical simulation in a micro-scale unit cell [7] and *(right)* using Gebart's model [6].

Permeability can also be estimated from numerical simulations, by asessing how pressure and velocity vary in a Stokes flow across a representative portion of porous medium. These models are often quite costly in computational terms, and raise the question of what a representative elementary volume should be in each situation.

Compressibility of reinforcements

In the previous section, we discussed the geometric origin of permeability. This raises the question of how a geometric and/or topological modification of the porous medium would affect its permeability. It has implications on multiple stages of composites manufacturing,

and could for instance be included in macroscopic flow models to account for any eventual movement of the fibers (see Terzaghi's principle, Biot's tensor and poromechanics). Most often, it is considered that the fibers do not move during impregnation.

However most processes involve a *forming* step (often by closing a mold) on dry reinforcements. Depending on the details of this forming process (applied force, displacement, creep, cycling, dynamic loading...), multiple geometric configurations can be obtained, and therefore the preform permeability can be marginally controlled. Being among the most common and influential modes of deformation, compression has been especially studied (Figure 11).

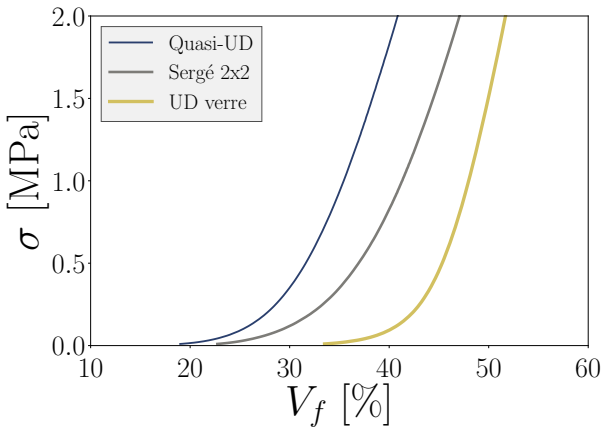

FIGURE 11: Evolution of the compressive stress σ with V_f with various flax and glass fabrics [11].

The mechanics of fibrous media thus constitutes an active research topic. It can be studied by direct experiments or numerical simulations (Figure 12), and while several theoretical models exist, they tend to be limited to very specific configurations while making strong hypotheses.

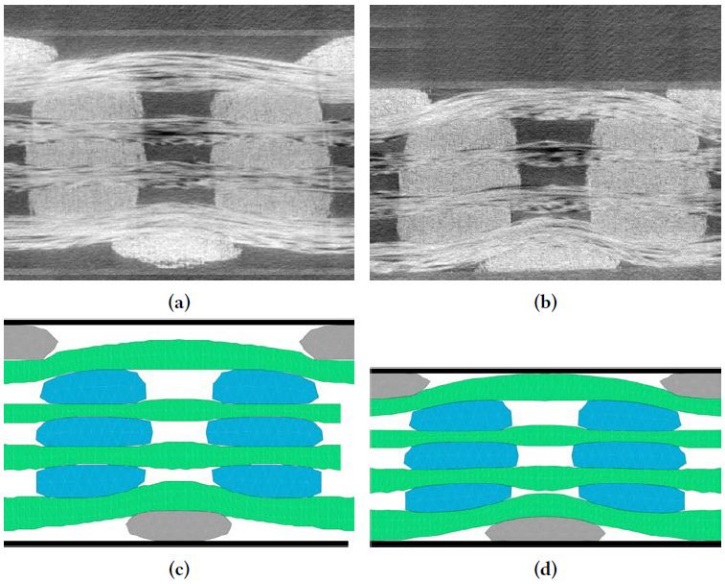

FIGURE 12: 2D cross-sections of a 3D fabric from X-ray CT (a, b) and numerical simulations (c, d), before (a, c) and after compression (b, d) [9].

Other considerations

There are yet many more details and phenomena which could be explored for the proper modeling of LCM processes. Some examples include chemical and physical modifications of fibers (roughness, surface treatment), the influence of resin rheology (non-newtonian flows), the kinetics of polymerization during impregnation, heat transfers...

References

[1] J. Bear. *Dynamics of Fluids in Porous Media*. Courier Corporation, 1972. 396 pp. ISBN: 978-0-486-65675-5.

[2] M. Bodaghi, S. V. Lomov, P. Simacek, N. C. Correia, and S. G. Advani. "On the variability of permeability induced by reinforcement distortions and dual scale flow in liquid composite moulding: A review". In: *Composites Part A: Applied Science and Manufacturing* 120 (2019), pp. 188–210. ISSN: 1359-835X. DOI: 10.1016/j.compositesa.2019.03.004.

[3] D. Bonn, J. Eggers, J. Indekeu, J. Meunier, and E. Rolley. "Wetting and spreading". In: *Reviews of modern physics* 81.2 (2009), p. 739.

[4] J. Castro, F. Sket, L. Helfen, and C. González. "In situ local imaging and analysis of impregnation during liquid moulding of composite materials using synchrotron radiation computed laminography". In: *Composites Science and Technology* 215 (2021), p. 108999. ISSN: 0266-3538. DOI: 10.1016/j.compscitech.2021.108999.

[5] R. G. Cox. "The dynamics of the spreading of liquids on a solid surface. Part 1. Viscous flow". In: *Journal of Fluid Mechanics* 168 (1986), pp. 169–194. ISSN: 1469-7645, 0022-1120. DOI: 10.1017/S0022112086000332.

[6] B. Gebart. "Permeability of Unidirectional Reinforcements for RTM". In: *Journal of Composite Materials* 26.8 (1992), pp. 1100–1133. ISSN: 0021-9983. DOI: 10.1177/002199839202600802.

[7] A. Geoffre. "Upscaling transient flows in fibrous multi-scale structures for infusion-based stochastic process modelling of composite structures". Thèse de doctorat. Saint-Etienne, EMSE, 2022.

[8] V. Michaud. "A Review of Non-saturated Resin Flow in Liquid Composite Moulding processes". In: *Transport in Porous Media* 115.3 (2016), pp. 581–601. ISSN: 1573-1634. DOI: 10.1007/s11242-016-0629-7.

[9] N. Naouar. "Analyse mésoscopique par éléments finis de la déformation de renforts fibreux 2D et 3D à partir de microtomographies X". Thèse de doctorat. INSA de Lyon, 2015.

[10] C. H. Park and W. I. Lee. "Modeling void formation and unsaturated flow in liquid composite molding processes: a survey and review". In: *Journal of Reinforced Plastics and Composites* 30.11 (2011), pp. 957–977. ISSN: 0731-6844. DOI: 10.1177/0731684411411338.

[11] V. Rougier. "Modélisation multi-échelle de l'imprégnation d'un milieu fibreux : morphologie, mouillage et perméabilité". Thèse de doctorat. Caen, Le Havre: Normandie Université, 2021.

[12] D. Salvatori, B. Caglar, H. Teixidó, and V. Michaud. "Permeability and capillary effects in a channel-wise non-crimp fabric". In: *Composites Part A: Applied Science and Manufacturing* 108 (2018), pp. 41–52. ISSN: 1359-835X. DOI: 10.1016/j.compositesa.2018.02.015.

[13] J. H. Snoeijer and B. Andreotti. "Moving Contact Lines: Scales, Regimes, and Dynamical Transitions". In: *Annual Review of Fluid Mechanics* 45.1 (2013), pp. 269–292. ISSN: 0066-4189, 1545-4479. DOI: 10.1146/annurev-fluid-011212-140734.

[14] H. Teixidó, J. Staal, B. Caglar, and V. Michaud. "Capillary Effects in Fiber Reinforced Polymer Composite Processing: A Review". In: *Frontiers in Materials* 9 (2022). ISSN: 2296-8016.

[15] H. N. Vo, M. F. Pucci, S. Corn, N. Le Moigne, W. Garat, S. Drapier, and P. J. Liotier. "Capillary wicking in bio-based reinforcements undergoing swelling – Dual scale consideration of porous medium". In: *Composites Part A: Applied Science and Manufacturing* 134 (2020), p. 105893. ISSN: 1359-835X. DOI: 10.1016/j.compositesa.2020.105893.